SEMI-PASSIVE CONTROL OF LINEAR AEROELASTIC VIBRATIONS USING SHUNTED PIEZOELECTRIC MATERIALS

Douglas D'Assunção
Department of Aeronautical Engineering, Engineering School of São Carlos, University of São Paulo, São Carlos SP, 13566-590, Brazil
douglasdassuncao@usp.br

Carlos De Marqui Júnior
Department of Aeronautical Engineering, Engineering School of São Carlos, University of São Paulo, São Carlos SP, 13566-590, Brazil
demarqui@sc.usp.br

Abstract. In this paper, semi-passive control techniques using piezoelectric shunts are experimentally investigated. The main motivation is the attenuation of linear aeroelastic oscillations. An airfoil with plunge and pitch degrees of freedom (DOF) is investigated. Piezoelectric coupling is introduced to the plunge DOF. Two different control schemes are presented. The Synchronized Switch Damping on Short (SSDS) technique is first investigated. The system is kept at the open circuit condition until a local extrema of mechanical displacement occurs. At this point the system switched to short-circuit condition, discharging the piezoceramics. Later, the circuit is re-switched to open-circuit until another displacement extrema occurs. Therefore, the power dissipation is maximized as well as the resistive shunt damping effect. The Synchronized Switch Damping on Inductor (SSDI) technique is also investigated in this paper. The system switched when a local maximum displacement occurs leading to the inversion of the voltage signal. In this case, the frequency of electrical resonance is larger than the frequency of mechanical oscillations, reducing the required inductance. This is important characteristic for aeroelastic systems, where the frequencies are usually low. An autonomous switching circuit (that does not requires external source of energy) is presented resulting in a self-powered flutter controller.

Keywords: semi-passive control, piezoelectric, aeroelasticity, shunt damping

1. INTRODUCTION

The use of smart materials in vibration control problems has increased in the last years. The main goal is to attenuate vibrations and improve the resistance to fatigue of an engineering system and the general performance of their functions. Although different smart materials are available, the piezoelectric one has received great attention in the last years. The main reasons are the sensing and actuation capabilities of piezoelectric material due to the direct and converse piezoelectric effects, respectively, as well as ease of application.

In general, the main control techniques using piezoelectric materials are the passive and active ones. In active control applications, piezoelectric material is used as actuator (converse piezoelectric effect). An input voltage is applied to the piezoelectric material and mechanical strain is produced in order to reduce unwanted vibrations (Fuller and Elliot, 1996). Sensors and external source of energy are required. In passive case, the piezoelectric material is shunted to a passive electrical circuit where the mechanical energy converted to electrical energy (direct piezoelectric effect) is dissipated. The first applications from shunt damping literature are reported as a resistive circuit (Uchino and Ishii, 1988), the inductive shunt circuit (Forward, 1979), the resistive-inductive in series (Hagood and von Flotow, 1991) and the resistive-inductive in parallel (Wu, 1996).

The literature of aeroelastic control also presents piezoelectric based vibration control investigations. Heeg (1993) reports the use of piezoceramics as actuators for flutter suppression of a rigid wing mounted on a flexible system. The flutter speed of the wind tunnel device was increased by 20% when the control loop was closed. The control of dynamic aeroelastic phenomena was demonstrated in the Piezoelectric Aeroelastic Response Tailoring Investigation (PARTI) conducted at NASA Langley Transonic Tunnel (McGowan *et al.*, 1998). A composite plate like wing with 36 piezoceramic patches was used and an increase of 12% in flutter dynamic pressure as well as 75% reduction of gust bending moment was achieved. Another widely known program is the Actively Controlled Response of Buffet Affected Tails (ACROBAT). Different authors investigate the use of piezoelectric actuators to damp tail buffeting of the F/A-18 aircraft (Moses, 1997; Moses, 1999; Hopkins *et al.*, 1998; Durr *et al.*, 1999). Giurgiutiu (2000) presents a comprehensive review of smart materials solutions for aeroelastic control in fixed wings and helicopters.

Although the literature demonstrates the successful use of piezoelectric actuators in active aeroelastic control some issues have to be addressed: the large amount of power required, the added hardware as well as control law design and implementation (McGowan, 1999). An alternative approach is the use of passive control to damp a single mode or a number of modes (Fleming and Moheimani, 2005). In such case, an external source of energy is not required, and simple electrical circuitry can be used. A few papers report the use of passive control schemes to damp aeroelastic

ISSN 2176-5480

D. D'Assunção, C. De Marqui Jr.
Semi-passive Control of Linear Aeroelastic Vibrations Using Shunted Piezoelectric Materials

oscillations. McGowan (1999) examines the performance of shunted piezoelectrics to reduce the aeroelastic response of a two-degree-of-freedom typical airfoil section. The aeorelastic equations with shunted piezoelectrics (resistive-inductive in parallel) are presented and the Theodorsen model used to determine the unsteady aerodynamic loads. The aeroelastic analysis shows that passive shunt damping circuits may provide a simple and effective method of subcritical aeroelastic oscillations control. Agneni *et al.* (2003) presents the modal-based modeling and analysis of the effectiveness of resistive-inductive shunted piezoelectric materials to damp aeroelastic systems. A weak performance of the passive controller in improving the stability margin (flutter envelope) of a composite wing of an unmanned glider is reported. However, the authors also report the ability of the passive devices to reduce the gust response amplitude of the wing in the neighborhood of flutter speed.

Since the frequencies of aeroelastic oscillations are very low (typically under 20Hz) the required inductances in passive control are extremely large and not practical. The use of synthetic inductance circuits (Riordan, 1967) is an alternative to address this issue. However, the internal resistance of such circuits might reduce the performance of passive controllers (Park and Inman, 2003). The Synchronized Switch Damping (SSD) techniques (Richard *et al.*, 1999, 2000; Clark, 2000; Guyomar *et al.*, 2007; Corr and Clark, 2002) can address the issues of passive controllers (associated with large inductance required in aeroelastic cases) and related to the complexities of active controllers. The SSD techniques are semi-passive methods that introduce the nonlinear treatment of the voltage output of the piezoelectric elements and induce an increase in mechanical to electrical energy conversion. In the semi-passive methods the piezoelectric material is kept in open circuit condition (maximum voltage output) except for a small period of time where voltage is canceled due to switch to small resistance (SSDS – synchronized switch damping on short-circuit) or inverted (SSDI – synchronized switch damping on inductor) due to brief switch to a resonant circuit. In both cases switching is performed synchronously with mechanical displacement. In the SSDS case, electrical energy is dissipated during voltage cancelation at short circuit condition resulting in increased damping effect. In the SSDI case, the required inductance is reduced if compared to the passive cases since it is related to electrical frequency and not related to mechanical oscillations. A more detailed discussion related to the semi-passive methods is presented in the next session.

The applications of semi-passive methods presented in the literature are limited to stable cases (electromechanical systems under external forces). This paper examines the experimental feasibility of using semi-passive methods to damp flutter oscillations of a typical section with pitch and plunge degrees of freedom (DOF). The piezoelectric coupling is added to the plunge DOF. Two different semi-passive methods are investigated in this paper. The SSDS and SSDI methods are employed to reduce linear aeroelastic response of the typical section at the flutter speed and also at post-flutter condition. In general, since external power is required to the switch (not to the piezoelectric element) these methods are named semi-passive ones. In this work however, the self-powered switching circuit presented by Richard *et al.* (2007) is employed and, therefore, a self-powered flutter controller is obtained.

2. SEMI-PASSIVE METHODS

The literature includes semi-passive methods (Richard *et al.*, 1999, 2000; Clark, 2000; Guyomar *et al.*, 2007; Corr and Clark, 2002) presented in order to overcome the previously mentioned drawbacks of purely passive and active controllers. The nonlinear treatment of the electrical output of an electroelastic system increases the mechanical to electrical conversion and consequently the shunt damping effect. In this section, the SSDS and SSDI methods as well as the switching circuit are presented and discussed. Both methods are used in the experimental tests of this paper. It is important to remember that different semi-passive methods are also included in the literature (Clark, 2000; Corr and Clark, 2002) but not discussed in this section.

The SSDS method, originally presented by Richard *et al.* (1999), consists in leaving the piezoelectric element in open circuit condition (electrical boundary condition that gives maximum voltage output) except when a local maximum voltage is detected. At this point, the system is switched to short-circuit condition for a small period of time. In the SSDI method, presented by Richard *et al.* (2000), when a local maximum is detected, the system is switched on inductor L, occurring the inversion of the voltage of the piezoelectric material. This inversion is due to a change in the voltage frequency when the inductor (L) is connected to the capacitance of the piezoelectric element (C_p). During the voltage inversion a resonant circuit LC_p is obtained and the inversion time is given by half pseudo-period Δt_i of the electrical network (Lallart *et al.*, 2008).

$$\Delta t_i = \pi \sqrt{LC_p} \tag{1}$$

Therefore, the inversion time is directly proportional to the inductance L, which in practical, must be chosen in such way that the frequency of the electrical resonant circuit (f_n), obtained during the switch, is 10 to 50 times the resonance frequency of the structure (Mohammadi, 2008).

In the SSDI case, the voltage after the inversion ($V(t)$) has an absolute value lower than the initial voltage (V_0), since the inversion is associated to electrical quality factor Q given as,

$$Q = \frac{L\omega_n}{R_i} = \frac{1}{R_i}\sqrt{\frac{L}{C_p}} \tag{2}$$

where R_i is the internal resistance of the switching circuit and ω_n is the resonance frequency of the circuit. The voltage inversion can be measured by defining an inversion coefficient γ. The constitutive equation of the *RLC* circuit is

$$\ddot{I}(t) + \frac{R_i}{L}\dot{I}(t) + \frac{1}{R_t C}I(t) = 0 \tag{3}$$

and one can obtain the voltage output of the electrical network as,

$$V(t) = V_0\left(-\frac{\omega_n}{2Q}t\right)\cos(\omega_1 t) \qquad \omega_1 = \sqrt{\omega_n^2 - \left(\frac{R_i}{2L}\right)^2} \tag{4}$$

Then, employing Eq. (1) and (2) into Eq. (4) yields

$$V(t) = -V_0 e^{\frac{\pi}{2Q}} = -\gamma V_0 \tag{5}$$

where γ is the inversion coefficient. The negative sign in Eq. (5) shows that the voltage is inverted. Since the inversion coefficient is related to the electrical quality factor (Q), the SSDS can be treated as a particular case of the SSDI with quality factor zero and, consequently, inversion coefficient is zero too (Mohammadi, 2008).

3. EXPERIMENTAL SET UP

In this paper, semi-passive techniques are experimentally investigated in aeroelastic control cases. An electromechanically coupled aeroelastic typical section is used in the experiments. Two techniques are investigated, the synchronized switching damping on short and the synchronized switching damping on inductor. An autonomous switching circuit (that does not requires external source of energy) is presented resulting in a self-powered flutter controller.

3.1 Typical section

Figure 1a shows the schematic of a linear 2-DOF typical section. The plunge and pitch displacement variables are denoted by h and α, respectively. The plunge displacement is measured at the elastic axis, i.e., at point P (positive downward) and the pitch angle is measured about the elastic axis (positive clockwise). In addition, b is the semichord of the airfoil section, x_α is the dimensionless chord-wise offset of the elastic axis from the centroid (C), k_h is the stiffness per length in the plunge DOF, k_α is the stiffness per length in the pitch DOF, d_h is the damping coefficient per length in the plunge DOF, d_α is the damping coefficient per length in the pitch DOF, and U is the airflow speed. In this work, electromechanical coupling is added to the plunge DOF. This way, the schematic of the electroaeroelastic section is shown in Fig. 1b. Aeroelastic vibrations of the cantilever (plunge spring) strain the piezoelectric patches dynamically and produces the electrical output.

D. D'Assunção, C. De Marqui Jr.
Semi-passive Control of Linear Aeroelastic Vibrations Using Shunted Piezoelectric Materials
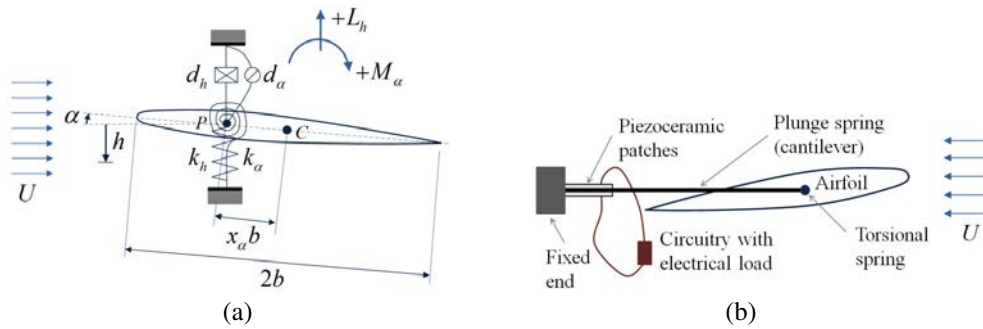

Figure 1. Aeroelastic typical section under airflow excitation (a) and Electroaeroelastic typical section with piezoelectric coupling on the plunge DOF and an external electrical load (b).

Figure 2 shows the experimental setup used for investigating the linear piezoaeroelastic behavior of the typical section. This setup is a typical aeroelastic section modified with piezoelectric coupling. The plunge stiffness is due the four elastic beams with clamped-clamped end conditions. The free ends of the elastic beams are connected to metal plates at the top and the bottom. A shaft (or pitch axis) is mounted to the upper and the lower plates through a pair of bearings. The pitch stiffness is given by a spring wire clamped into the shaft (at the elastic axis), shown in the enlarged view of figure 2b. The free end of the wire is simply supported on the top plate. Two piezoceramic patches (QP10N from Mide Technology Corporation) are attached onto the root of two bending stiffness members (symmetrically) and their electrodes are connected in parallel to the external resistive load. The table 1 shows the experimental parameters of the typical section used in this paper.
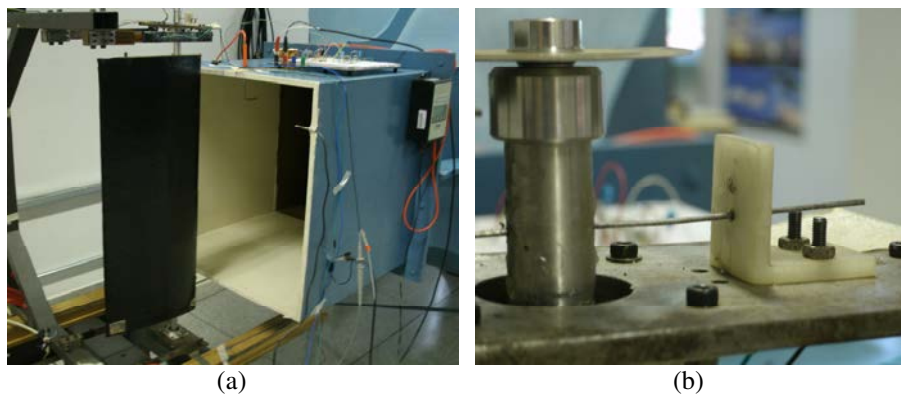

Figure 2. Experimental typical section (a) and detailed view of the pitch spring (b).

The plunge displacement (h) is measured by using a strain gage bonded on the beam, on a ¼ bridge configuration. The pitch displacement (α), is measured with a digital encoder US, model HEDS-9000-T00, attached to the aluminum axis of the wing. The acquisition of all data was performed with a dSPACE® DS1104 system.

Table 1. Experimental parameters of the typical section.

Parameter	Value	Unit
b	1.25×10^{-1}	m
$x_a b$	3.2×10^{-1}	kg/m
m	1.542	kg/m
m_e	2.548	kg/m
I_a	7.2×10^{-3}	kg.m
k_a	5.08	N/rad
k_h	4.2×10^{3}	N/m^2
d_a	6.35×10^{-2}	N.s/rad
d_h	1.8146	N.s/rad^2
θ	1.55×10^{-3}	N/V
C_p	85×10^{-9}	F

3.2 Self-powered electronic breaker circuit

The electronic circuit breaker used in this paper is based on the circuit proposed by Richard et al. (2007) and Zhu *et al.*, (2012). Passive electronic components are used and three basic functions are addressed: an envelope detector (R1, C1, D1), a comparator (R2, D2, Q1) and a switch (D3, R3 and Q2), where R is a resistor, C a capacitor, D a diode and Q a transistor, as shown in Fig. 3.

The envelope detector is a low-pass filter whose output amplitude should be very similar to the voltage piezoelectric signal with a small phase delay. The comparator circuit (R2, D2, Q1) compares the filter output signal on C1 with the voltage of the piezoelectric material. Thus, while the voltage amplitude of the envelope is smaller than the voltage of the piezoelectric, the transistor Q1 is blocked. When the piezoelectric voltage is higher than the voltage of the envelope, and the difference between the envelope voltage and piezoelectric voltage is larger than the threshold of the transistor Q1, it is conducted. Consequently, the transistor Q2 is triggered and the switching process is started. Accordingly, the minima switch is performed in a similar way, with different polarities of diodes and transistors given in Fig. 4.
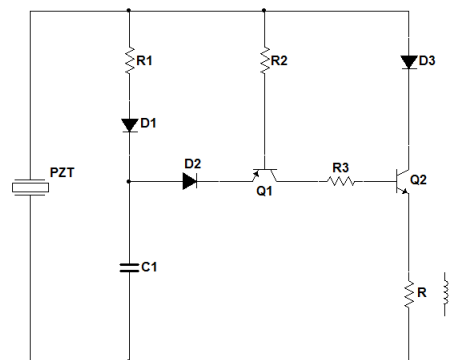

Figure 3. Circuit diagram of self-powered electronic breaker

Both maximum electronic breaker and minimum electronic breaker are combined to give the complete system of Figure 4. The voltage output obtained during the aeroelastic experiments is high enough to take the transistors Q2 and Q3 into saturation mode simultaneously. This behavior caused a malfunction of the circuit breaker. The diodes D7 and D8 were then used in order to avoid this issue and to ensure independent operation of the transistors Q2 and Q3.
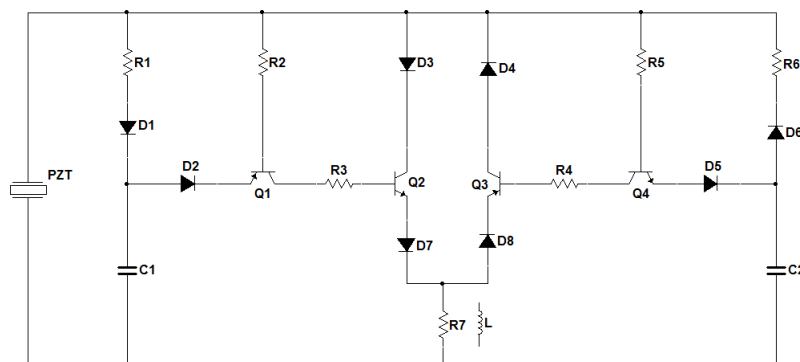

Figure 4. Circuit diagram of the self-powered full-wave electronic breaker

In this paper, the same electronic circuit breaker is used for the SSDS and SSDI cases. The difference is to use a R7=100 Ω for the SSDS case and L=8 H (and internal resistance of 505 Ω) for the SSDI case, as shown in Fig. 4. Table 2 shows the values of electrical components for the self-powered electronic breaker circuit.

Table 2. Electrical components values for self-powered electronic breaker.

D1 to D8	Diodes fast soft-recovery	BYW95C
Q1 and Q3	Transistor – PNP high voltage amplifier	MPSA92
Q2 and Q4	Transistor – NPN high voltage amplifier	MPSA42

R1 and R6	Resistor	1 kΩ
R1 to R6	Resistor	10 kΩ

4. RESULTS AND DISCUSSION

In this section, the SSDS and SSDI methods are employed to reduce linear aeroelastic response of the typical section at the flutter speed and also at post-flutter condition.

The linear flutter speed of the electromechanically coupled typical section was experimentally determined considering the piezoceramics in open circuit condition. The flutter speed was estimated by testing the system at various airflow speeds. An initial condition was applied to the linear displacement DOF (plunge) and free response of the system measured. Figure 5 presents the time histories of voltage, pitch and plunge displacements for an airflow speed of 11.7 m/s. Note that the time histories of pitch and plunge displacements exhibits a decaying behavior. Figure 6 presents the time histories of voltage, pitch and plunge displacements for the airflow speed of 11.9 m/s. At this airflow speed the typical linear flutter behavior with persistent oscillations and increasing amplitude is observed. Therefore, the airflow speed of 11.9 m/s is assumed as the linear flutter speed (open circuit condition).
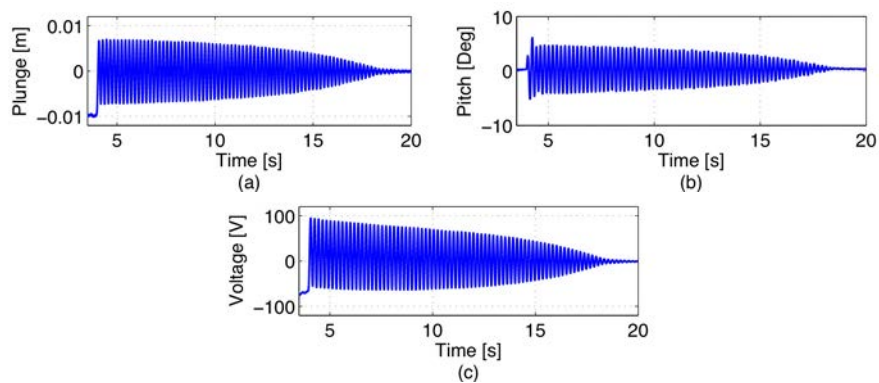

Figure 5. Time histories of plunge displacements (a), pitch displacement (b) and voltage (c), under airflow speed of 11,7 m/s
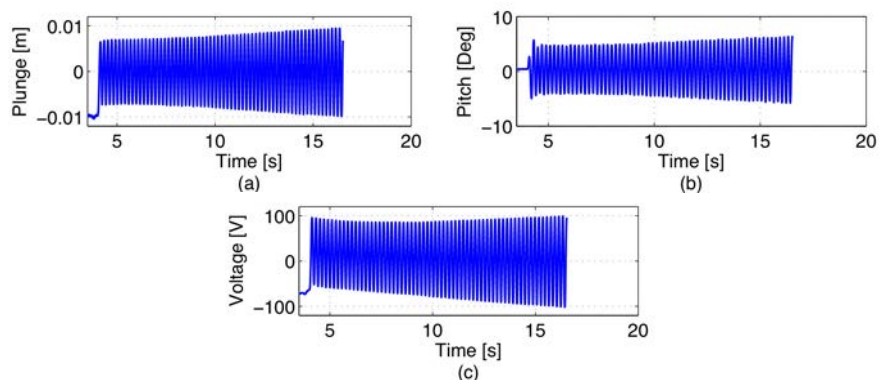

Figure 6. Time histories of plunge displacements (a), pitch displacement (b) and voltage (c), under airflow speed of 11,9 m/s

The experimental investigation of flutter suppression of the typical section by using the SSDS and SSDI schemes is also presented. In the wind tunnel experiments, an initial displacement was applied to the plunge DOF for the flutter speed. In the two cases (SSDS and SSDI), the piezoceramics were in open circuit condition for the ten initial seconds, when they were connected to the self-powered electronic breaker. Figure 7 shows the time histories of pitch, plunge and voltage output for the linear flutter speed and SSDS control scheme. As can be observed in Fig 7, after the piezoceramics are attached to the switching circuit, the mechanical and electrical oscillations decay and are suppressed in 8 seconds. Figure 8 shows the time histories of pitch, plunge and voltage output for the linear flutter speed and SSDI control scheme. As can be observed in Fig 8, after the piezoceramics are attached to the switching circuit, the mechanical and electrical oscillations decay and are suppressed in 6 seconds.
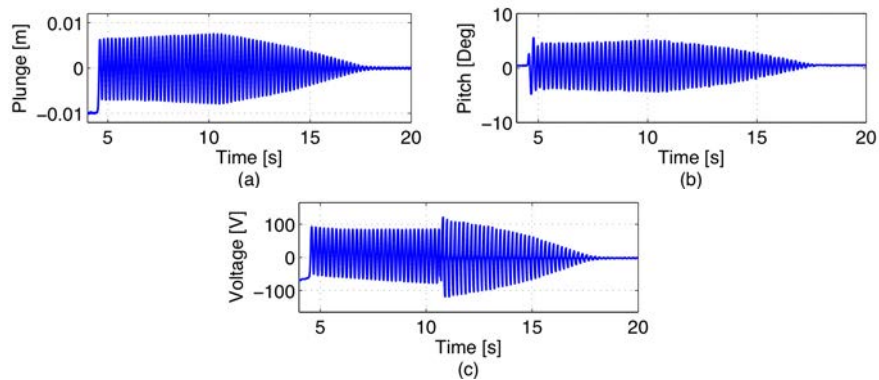
Figure 7. Time histories, using SSDS, of plunge displacements (a), pitch displacement (b) and voltage (c), at the linear flutter speed
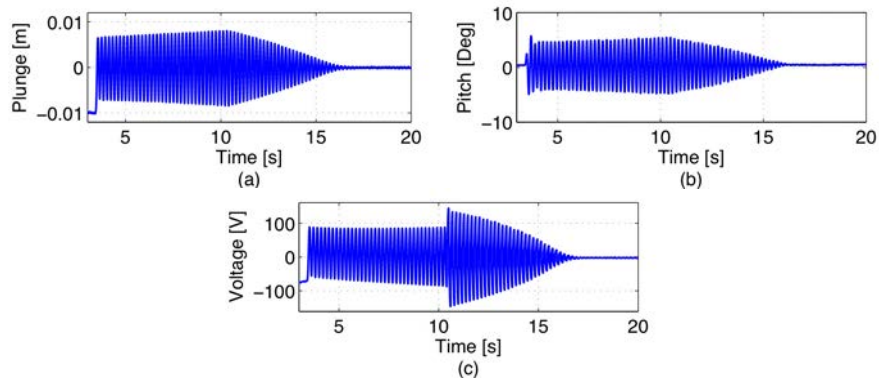

Figure 8. Time histories, using SSDI, of plunge displacements (a), pitch displacement (b) and voltage (c), at the linear flutter speed

Figure 9 shows the detailed view of the switching process for the voltage output of the cases presented in Figures 7 and 8. The piezoelectric material is kept in open circuit condition except for a small period of time (when the switch is closed). Figure 9a shows that the switch is closed for the quarter of oscillating period when the voltage reaches an extremum. While the switch is closed the voltage drops to zero. The time history of voltage output for the SSDI case is shown in Fig. 9b. One should note that the voltage inversion is not complete. This is due to the internal resistance of the switching circuit and internal resistance of the inductor. By using the equation 5, the inversion coefficient obtained in the experiments is 0.25 and the electric quality factor is 1.13.
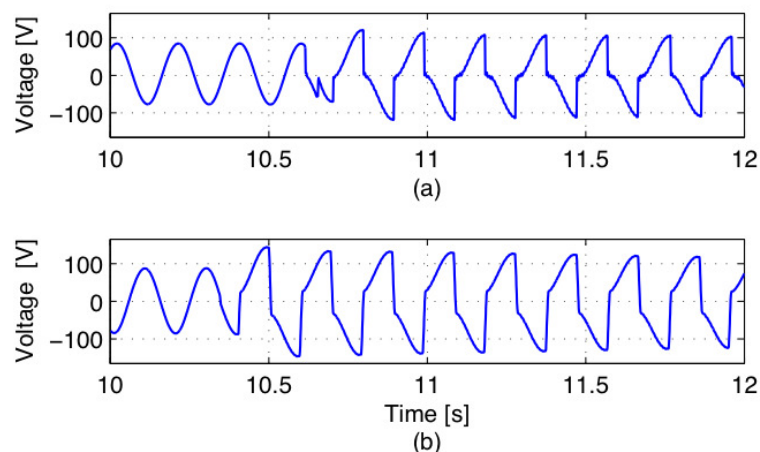

Figure 9. Detailed view of the electrical response after triggering the circuit breaker: (a) Using SSDS; (b) Using SSDI

D. D'Assunção, C. De Marqui Jr.
Semi-passive Control of Linear Aeroelastic Vibrations Using Shunted Piezoelectric Materials

In another experiment, it was analyzed the performance of the two semi-passive systems at the post flutter condition. In both cases (SSDS and SSDI), the piezoelectric remain connected to the circuit breaker and the systems are tested for airflow speeds larger then the flutter speed. When the SSDS technique was used (Figure 10), the flutter oscillations were suppressed until the airflow speed of 12.7 m/s. For airflow speeds larger than 12.7 m/s the typical flutter behavior was observed, as shown in Fig. 11. It is important to note that the flutter speed is 8.5 % larger then the open circuit flutter speed when the SSDS control is used.
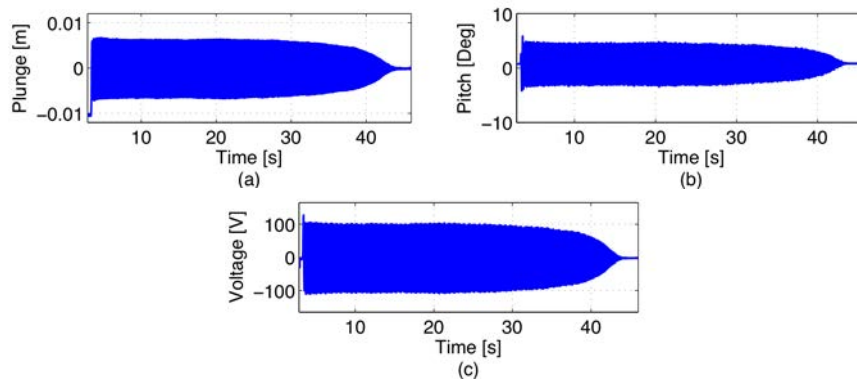

Figure 10. Plunge displacements (a), pitch displacement (b) and voltage (c) using SSDS, under 12.7 m/s airflow speed
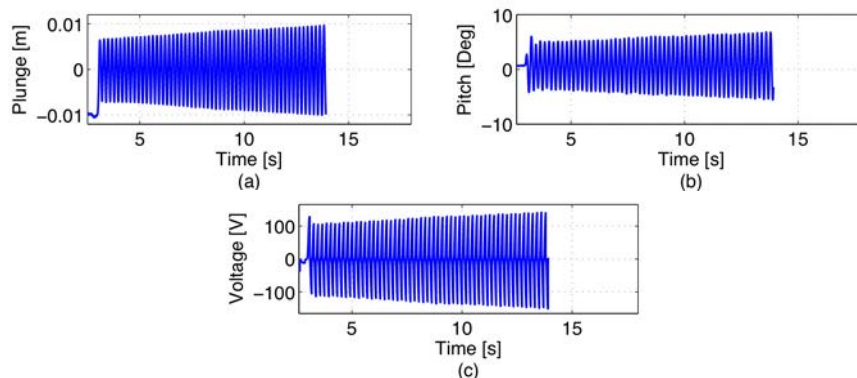

Figure 11. Plunge displacements (a), pitch displacement (b) and voltage (c) using SSDS, under 12.8 m/s airflow speed

When the SSDI technique was used (Figure 12), the flutter oscillations were suppressed until the airflow speed of 13.1 m/s. For airflow speeds larger than 13.1 m/s the typical flutter behavior was observed, as shown in Fig. 13. It is important to note that when the SSDI control is used the flutter speed is 11.4% larger then the open circuit flutter speed.
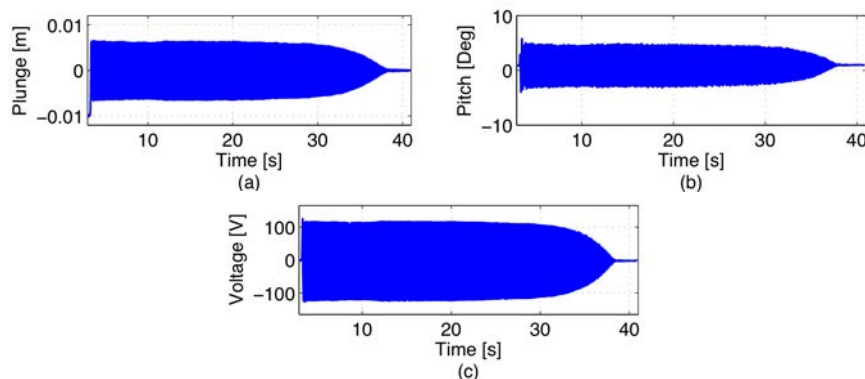

Figure 12. Plunge displacements (a), pitch displacement (b) and voltage (c) using SSDI, under 13.1 m/s airflow speed
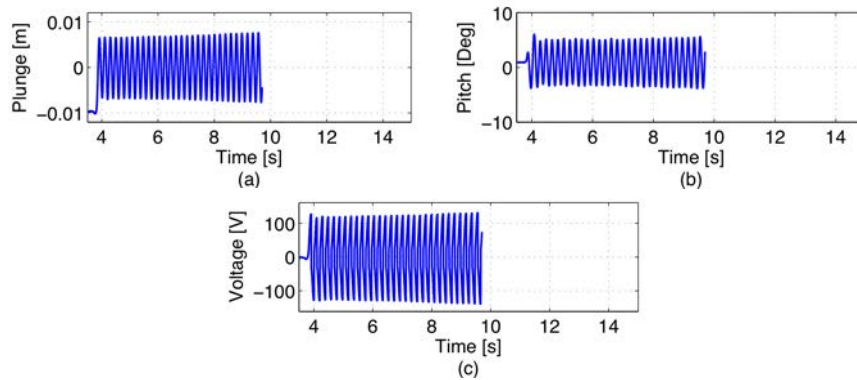
Figure 13. Plunge displacements (a), pitch displacement (b) and voltage (c) using SSDI, under 13.2 m/s airflow speed

5. CONCLUSIONS

In this paper, self-powered piezoelectric flutter controllers (using self-powered switching circuit) were presented. Flutter oscillations were successfully suppressed during the experiments and no external energy is required by the control system. The linear flutter speed of the electromechanically coupled typical section was measured as 11.9 m/s, with piezoceramic in open circuit condition. Flutter oscillations were successfully suppressed when both SSDS and SSDI control schemes were tested. However, a better performance is observed for SSDI control. This is due the voltage inversion observed in the SSDI case. This inversion provides a mechanical dissipative force in the aeroelastic system. The linear flutter speed of the typical section was increased by 8.5% and 11.4% for the SSDS and SSDI cases, respectively. The semi-passive techniques presented in this paper for aeroelastic control are interesting alternatives to the passive piezoelectric controllers previously investigated in the literature. An issue related to the required inductance in passive controllers was addressed and a good control performance achieved at the flutter condition as well as in post flutter regime.

6. ACKNOWLEDGEMENTS

7. REFERENCES

Agneni, A.; Mastroddi, F.; Polli, G. M. Shunted piezoelectric patches in elastic and aeroelastic vibrations. *Computers & Structures*, v. 81, n. 2, p. 91–105, 2003.

Clark, W. W. Vibration Control with State-Switched Piezoelectric Materials. *Journal of Intelligent Material Systems and Structures*, v. 11, n. 4, p. 263–271, 2000.

Corr, L. R.; Clark, W. W. Comparison of low-frequency piezoelectric switching shunt techniques for structural damping. *Smart Materials and Structures*, v. 11, n. 3, p. 370–376, 2002.

Dürr, J. Integration of piezoceramic actuators in fiber-reinforced structures for aerospace applications. *Journal of Intelligent Material Systems and Structures*, v. 3326, p. 81–92, 1998.

Fleming, A. J.; Moheimani, S. O. R. Control orientated synthesis of high-performance piezoelectric shunt impedances for structural vibration control. *IEEE Transactions on Control Systems Technology*, v. 13, n. 1, p. 98–112, 2005.

Forward, R. L. Electronic damping of vibrations in optical structures. *Applied Optics*, v. 18, n. 5, p. 690, 1979.

Fuller, C. C.; Elliott, S.; Nelson, P. A. *Active control of vibration*. 1st edition ed. San Diego, CA: Academic Press, 1996.

Giurgiutiu, V. Review of Smart-Materials Actuation Solutions for Aeroelastic and Vibration Control. *Journal of Intelligent Material Systems and Structures*, v. 11, n. 7, p. 525–544, 2000.

Guyomar, D.; Richard, C.; Mohammadi, S. Semi-passive random vibration control based on statistics. *Journal of Sound and Vibration*, v. 307, n. 3-5, p. 818–833, 2007.

Hagood, N. W.; Von Flotow, A. Damping of structural vibrations with piezoelectric materials and passive electrical networks. *Journal of Sound and Vibration*, v. 146, n. 2, p. 243–268, 1991.

Heeg, J. Analytical and Experimental Investigation of Flutter Suppression by Piezoelectric Actuation. *NASA Technical Paper* 3241, 1993.

Hopkins, M. A.; Henderson, D. A.; Moses, R. W. et al. Active vibration-suppression systems applied to twin-tail buffeting. In: J. M. Sater (Ed.); *SPIE*. v. 3326, p.27–33, 1998. San Diego, CA.

Lallart, M.; Lefeuvre, É.; Richard, C.; Guyomar, D. Self-powered circuit for broadband, multimodal piezoelectric vibration control. *Sensors and Actuators A: Physical*, v. 143, n. 2, p. 377–382, 2008.

McGowan, A. M. R. An examination of applying shunted piezoelectrics to reduce aeroelastic response. *CEAS/AIAA/ICASE/NASA Langley International Forum on Aeroelasticity and Structural Dynamics 1999*. p.553–572, 1999.

McGowan, A.; Wilkie, W. K.; Moses, R. W. et al. Aeroservoelastic and structural dynamics research on smart structures conducted at NASA Langley Research Center. *Proceedings of SPIE* - The International Society for Optical Engineering. v. 3326, p.188–201, 1998.

Mohammadi, S., 2008. *Semi-passive vibration control using shunted piezoelectric materials*. Thesis. Department of Electrical Engineering, Institut National des Sciences Appliquées de Lyon.

Moses, R. W. Vertical-tail-buffeting alleviation using piezoelectric actuators: some results of the actively controlled response of buffet-affected tails (ACROBAT) program. *Proceedings of SPIE* - The International Society for Optical Engineering. v. 3044, p.87–98, 1997.

Moses, R. W. Contributions to active buffeting alleviation programs by the NASA Langley Research Center. Collection of Technical Papers - *AIAA/ASME/ASCE/AHS/ASC Structures, Structural Dynamics and Materials Conference*. Anais... v. 2, p.1034–1042, 1999.

Park, C. H.; Inman, D. J. Enhanced piezoelectric shunt design. *Shock and Vibration*, v. 10, n. 2, p. 127–133, 2003.

Richard, C.; Guyomar, D.; Lefeuvre, E. Self-powered electronic breaker with automatic switching by detecting maxima or minima of potential difference between its power electrodes. *WO Patent*, Patent PCT/FR2005/003000, Publication number: WO/2007/063194, 2007.

Richard, C.; Guyomar, D.; Audigier, D.; Bassaler, H. Enhanced semi passive damping using continuous switching of a piezoelectric device on an inductor. In: V. V. Varadan; N. M. Wereley; R. O. Claus; et al. (Eds.); *Proceedings of SPIE* - The International Society for Optical Engineering. v. 3989, p.288–299, 2000.

Richard, C.; Guyomar, D.; Audigier, D.; Ching, G. Semi-passive damping using continuous switching of a piezoelectric device. (V. V. Varadan, N. M. Wereley, Y. Bar-Cohen, et al., Eds.) *Proceedings of SPIE* - The International Society for Optical Engineering, v. 3672, n. March, p. 104–111, 1999.

Riordan, R. H. S. Simulated inductors using differential amplifiers. *Electronics Letters*, v. 3, n. 2, p. 50, 1967.

Uchino, K.; Ishii, T. Mechanical damper using piezoelectric ceramics. *Nippon Seramikkusu Kyokai Gakujutsu Ronbunshi/Journal of the Ceramic Society of Japan*, v. 96, n. 8, p. 863–867, 1988.

Wu, S. Piezoeleciric shunts with a parallel R-L circuit for structural damping and vibration control. *Smart Structures and Materials 1996: Passive Damping and Isolation*. v. 27201259, p.259–269, 1996.

8. RESPONSIBILITY NOTICE

The authors are the only responsible for the printed material included in this paper.